

VR-Doh: Hands-on 3D Modeling in Virtual Reality

ZHAOFENG LUO*, Carnegie Mellon University, USA and Peking University, China

ZHITONG CUI*, Carnegie Mellon University, USA and Zhejiang University, China

SHIJIAN LUO, Zhejiang University, China

MENGYU CHU, Peking University, China

MINCHEN LI, Carnegie Mellon University, USA



Fig. 1. The figure demonstrates the intuitive and versatile capabilities of our VR-Doh system. In the upper row, users deform the vase and refine the roses with tools and gestures. The lower row showcases the system’s versatility, enabling seamless table deformation by hand contact, object removal, and vase placement. This workflow simplifies complex editing tasks, delivering realistic results efficiently and intuitively.

We introduce VR-Doh, a hands-on 3D modeling system that enables intuitive creation and manipulation of elastoplastic objects in Virtual Reality (VR). By customizing the Material Point Method (MPM) for real-time simulation of hand-induced large deformations and enhancing 3D Gaussian Splatting for seamless rendering, VR-Doh provides an interactive and immersive 3D modeling experience. Users can naturally sculpt, deform, and edit objects through both contact- and gesture-based hand-object interactions. To achieve real-time performance, our system incorporates localized simulation techniques, particle-level collision handling, and the decoupling of physical and appearance representations, ensuring smooth and responsive interactions. VR-Doh supports both object creation and editing, enabling diverse modeling tasks such as designing food items, characters, and interlocking structures, all resulting in simulation-ready assets. User studies with both novice and experienced participants highlights the system’s intuitive design, immersive feedback, and creative potential. Compared to existing geometric modeling

*Both authors contributed equally to this research.

Authors’ Contact Information: Zhaofeng Luo, Carnegie Mellon University, USA and Peking University, China, roushelfy@stu.pku.edu.cn; Zhitong Cui, Carnegie Mellon University, USA and Zhejiang University, China, zhitongcui@zju.edu.cn; Shijian Luo, Zhejiang University, China, sjluo@zju.edu.cn; Mengyu Chu, Peking University, China, mchu@pku.edu.cn; Minchen Li, Carnegie Mellon University, USA, minchernl@gmail.com.

tools, VR-Doh offers enhanced accessibility and natural interaction, making it a powerful tool for creative exploration in VR.

CCS Concepts: • **Computing methodologies** → **Virtual reality**.

Additional Key Words and Phrases: Virtual Reality, 3D Modeling, Elastoplasticity Simulation, Material Point Method, Human-Computer Interaction

1 INTRODUCTION

With the growing demand for digital content, there is an urgent need to address key challenges in 3D content creation: ease of use, scalability, efficiency, and quality. Traditional 3D modeling tools impose significant barriers for novice users, requiring expertise in real-world observation, specialized techniques, and iterative fine-tuning. This reliance on professional skills limits accessibility, hindering wider participation in high-quality content creation.

Meanwhile, 3D modeling in Virtual Reality (VR) has become increasingly popular due to its ability to provide immersion and depth, thereby enhancing designers’ creativity and collaboration [Rosales et al. 2019; Yu et al. 2021]. Commercial tools like Shapelab [sha 2025] and Gravity Sketch [gra 2025] have advanced this vision. However, their approaches are still limited to procedural methods, such as

drawing curves to form surfaces from scratch, which are restricted to geometric techniques and require significant skills.

In contrast, physics-aware shape modeling introduces a novel paradigm that aligns more closely with human intuition and natural interactions. In this approach, objects are simulated as deformable solids, reshaped through contact forces or boundary conditions specified by the user [Fang et al. 2021]. In the context of VR, using hands as an input modality is particularly compelling, as it mimics the way users naturally manipulate physical objects, such as clay. This approach leverages users’ prior experience with creating real-world objects, making the modeling process more intuitive and accessible [Arora et al. 2019; Pihuit et al. 2008; Schulz et al. 2019].

Building on these foundational advantages, we integrate physics-based simulation into VR to deliver an intuitive and efficient hands-on 3D modeling system, *VR-Doh*. Our primary objective is to enable users to create and edit virtual objects with a high degree of realism, leveraging direct hand-based contact and gestures alongside interactive feedback. To efficiently support large deformations and contact handling, we adopt the Material Point Method (MPM) [Hu et al. 2018; Jiang et al. 2016], a hybrid Lagrangian-Eulerian framework capable of simulating versatile elastoplastic materials.

VR-Doh enables users to create 3D models by deforming and composing built-in primitive geometries, with surface meshes reconstructed from MPM particles. Additionally, based on Xie et al. [2024], we extend support for editing existing 3D data represented by Gaussian Splatting (GS) [Kerbl et al. 2023], allowing content creation through the modification of realistically rendered objects captured from the real world. To achieve real-time responsiveness despite the computational demands of simulation and rendering, we introduce optimizations such as particle-level collision handling and the decoupling of appearance and physical representations, allowing detailed hand-object interactions within budgeted simulation degrees of freedom. Beyond hand-based contact and gestures, we integrate a suite of deformation tools driven by tracked hand motions, providing diverse and precise deformations to enhance users’ creative flexibility. To evaluate VR-Doh’s usability and effectiveness, we conducted user studies with participants of varying expertise. The study highlights its intuitive design, immersive feedback, and potential for complementing traditional modeling software in creative exploration. These findings offer insights into how users naturally leverage physics-based interactions, paving the way for future improvements and more immersive 3D modeling experiences in VR.

Our key contributions are summarized as follows:

- *A novel physics-based VR 3D modeling paradigm*: We present VR-Doh, a VR system that integrates physics-based simulations to deliver intuitive and immersive workflows, making 3D modeling more accessible to users of varying expertise.
- *Intuitive modeling through natural interactions*: VR-Doh uses hand-based contact and gesture inputs together with deformation tools to support tasks from basic shape editing to complex modeling, mimicking real-world interactions.
- *Real-time performance through technical innovations*: We ensure smooth and responsive interactions with optimizations such as localized simulation, decoupled appearance

and physical representations, and particle-level collision handling for efficient computation.

- *Comprehensive evaluation*: Extensive user studies and experiments validate VR-Doh’s effectiveness, offering insights into how physics-based hand-object interactions enhance intuitive and creative 3D modeling in VR.

A key advantage of our approach is its ability to make 3D modeling in VR significantly more intuitive and accessible, especially for novice users. By incorporating physics-based deformations, VR-Doh provides a realistic and immersive modeling experience that surpasses traditional geometric modeling approaches. Hands-on input lowers the barrier to entry, enabling users to interact with virtual objects naturally and intuitively, while flexible selection of operation areas improves efficiency and enhances immersion. This direct interaction mimics real-world manipulation, allowing users to predict outcomes based on everyday experiences and reducing the reliance on specialized skills and technical expertise.

2 RELATED WORK

Virtual Clay Modeling. Virtual modeling of clay-like materials using dexterous input offers significant advantages over traditional 3D modeling, including high expressivity and a lower learning curve, effectively replicating the tactile experience of working with physical clay [Chatterjee 2024; Sheng et al. 2006]. Despite these benefits, the computational demands of simulating dexterous hand-object interactions have limited the integration of virtual clay modeling into VR environments, with most existing implementations constrained to 2D screens. Early approaches to virtual clay modeling utilized dynamic subdivision solids [McDonnell et al. 2001], followed by the application of plasticity models to capture essential physical properties of real clay, such as mass conservation and surface tension effects [Dewaele and Cani 2004]. To improve interactivity, Barreiro et al. [2021] introduced a particle-based viscoplasticity model with ultrasound haptic feedback, although the fidelity of finger-based interactions remained insufficient for detailed 3D modeling tasks. Additionally, physical proxies have been employed to enhance the virtual clay experience [Marner and Thomas 2010; Sheng et al. 2006], such as combining direct finger input with deformable physical devices to enable clay-like sculpting operations, including deforming, smoothing, pasting, and extruding [Sheng et al. 2006]. Efforts to adapt virtual clay modeling to VR environments have been limited. For instance, Moo-Young et al. [2021] made preliminary attempts to integrate these techniques into VR; however, their approach faced challenges in achieving the robustness and accuracy needed for intricate hand-object interactions. To address this gap, our work introduces a realistic, hands-on modeling framework for VR, leveraging the Material Point Method [Jiang et al. 2016] and efficient hand-object contact handling to enable intuitive and detailed clay-like modeling in virtual environments.

Physics-Aware Interactions in VR. Physics-aware hand-object interactions in VR have been extensively studied, enabling users to engage with various virtual phenomena such as particle-based animations [Arora et al. 2019], deformable objects [Deng et al. 2023; Jiang et al. 2024; Moo-Young et al. 2021], and fluids [Eroglu et al. 2018]. These approaches often utilize hand-tracking data to map

human hand motions to rigged virtual hand models, enabling dynamic interactions in immersive environments. For example, Höll et al. [2018]; Kumar and Todorov [2015]; Lougiakis et al. [2024] use tracked hand information to define the pose of the virtual hand in each frame while incorporating frictional contact, achieving realistic hand-rigid-body interactions. Building on this, Jacobs and Froehlich [2011]; Smith et al. [2020]; Verschoor et al. [2018] simulate soft hands using nonlinear soft tissue models, which allow for more natural and realistic interactions. While these works primarily focus on interactions between hands and rigid objects, research on hand-deformable-object interactions has also gained traction. For instance, Deng et al. [2023] developed PhyVR, a unified particle system for freehand interactions with multiple virtual materials; VR-GS [Jiang et al. 2024] facilitates handle-based interaction with physically simulated elastic objects represented by 3D Gaussian Splatting [Kerbl et al. 2023]. However, these efforts largely emphasize physics-aware interactions rather than shape editing, which holds significant promise for creative tasks such as animation control [Arora et al. 2019]. To address this gap, we focus on physics-based hands-on 3D modeling in VR, leveraging both contact- and gesture-driven interactions to enable intuitive creation and editing of deformable objects for creative applications.

3D Modeling Tools in VR. Creative tools for 3D modeling in VR encompass different categories. Among drawing-based modeling tools, Surface Drawing [Schkolne et al. 2001] stands as a pioneering approach, enabling users to draw strokes in space using hand motions and edit 3D models with tangible tools. SurfaceBrush [Rosales et al. 2019] and AdaptiBrush [Rosales et al. 2021] convert dense collections of artist-drawn stroke ribbons into user-intended manifold free-form 3D surfaces. Cassie [Yu et al. 2021] is a conceptual modeling system in VR that leverages free-hand mid-air sketching and a novel 3D optimization framework to create a connected curve network. In addition, inspired by FiberMesh [Nealen et al. 2007], RodMesh [Schulz et al. 2019] replaces the curve drawing with two-handed bending and stretching of virtual rods, allowing users to define outline shapes that are subsequently inflated into manifold mesh surfaces. Commercial tools, such as Shapelab, Adobe Substance 3D Modeler¹, and Kodon², mainly focus on geometric editing through polygonal or voxel-based sculpting. These tools allow users to manipulate geometry regions and apply operations with dynamic topology updates. Notably, Gravity Sketch introduces subdivision modeling, enabling users to create complex meshes from simple base topology while maintaining smoothness. Inspired by these prior works, we aim to further reduce the demand for professional 3D modeling expertise with physics-aware hands-on shape modeling, making 3D modeling in VR more accessible to novice users.

3 DESIGN RATIONALE

To make hands-on 3D modeling in VR responsive, immersive, and user-friendly, we have derived the following design requirements and functionalities:

- (1) **Realistic Physics-based Simulation.** This provides users with an intuitive understanding of how their input translates

into deformations, offering a more intuitive shape modeling process compared to conventional desktop-based tools.

- (2) **Real-Time Performance.** Maintaining real-time frame rates and smooth rendering is crucial in VR to avoid motion sickness³, which severely impacts the user experience. Ensuring real-time responsiveness for shape deformations to hand input is essential for intuitive interactions.
- (3) **Diverse Input Modalities.** In real-world clay modeling, people combine hand manipulation with tools like ball styluses and knives for precise and controlled deformations. Supporting the use of various tools in VR, beyond just hand manipulation, would enhance efficiency and unlock more creative shape-modeling possibilities.
- (4) **Adhering to established operations.** Design is an iterative process, where complex models are often composed of multiple components. An effective modeling workflow should follow established operations, including creating, moving, scaling, merging, and copying individual objects, to achieve the final design.
- (5) **Intuitive Spatial Interface.** A clear and user-friendly spatial interface is critical to guide users through the modeling process and improve the overall usability of the system.

Simultaneously achieving all these goals presents a significant challenge. The more accurate the simulation and rendering, the greater the demand for computational resources. Appropriate input modalities are required to enable hands to deform virtual objects in mid-air as expected. In the following sections, we will explain how we built VR-Doh, including the overall system architecture, methodologies, and the technical trade-offs and innovations we employed.

4 METHOD

Our system, built on PhysGaussian [Xie et al. 2024], integrates intuitive user interactions, real-time simulation, and high-quality rendering to enable hands-on 3D modeling in VR. PhysGaussian combines the Moving Least Squares (MLS) Material Point Method (MPM) [Hu et al. 2018] and 3D Gaussian Splatting [Kerbl et al. 2023] for elastoplastic simulation and photorealistic rendering. The technical background of these foundational methods is provided in our supplemental document. However, directly applying these techniques does not fully address the challenges of enabling real-time performance, intuitive usability, and dynamic updates in our system. To overcome these limitations, we introduce key innovations, including particle-level collision handling and localized simulations for efficient and accurate modeling (subsection 4.2), as well as decoupled appearance and physical representations and uniform Gaussian volume regularization for enhanced rendering (subsection 4.3). These innovations, combined with natural interaction modes such as contact- and gesture-based inputs that mimic real-world actions (subsection 4.1), make VR-Doh both accessible to novice users and powerful for detailed modeling tasks. Figure 2 and Algorithm 1 provide an overview of the system framework.

¹<https://www.adobe.com/products/substance3d/apps/modeler.html>

²<https://www.kodon.xyz/>

³VR motion sickness: a condition where users experience nausea and discomfort due to mismatches between visual and physical motion

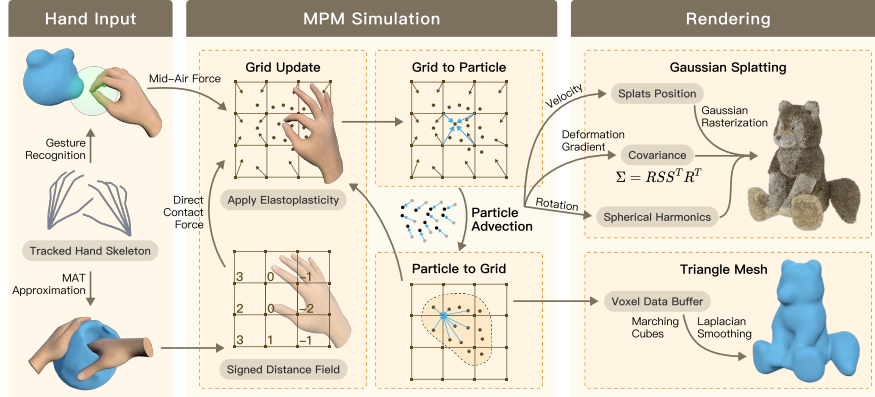


Fig. 2. **VR-Doh Pipeline.** Our interactive system enables hands-on 3D modeling in VR through contact- and gesture-based inputs. The pipeline integrates MPM to simulate realistic elastoplastic deformations and supports rendering using both 3D Gaussian Splatting and meshes, ensuring broad applicability across creative and practical modeling tasks.

Algorithm 1 VR-Doh Pipeline

```

1: while True do
2:   Update_Input()                                ▶ subsection 4.1
3:   for each substep do
4:     Sim_substep()                               ▶ Supp. Doc. and subsection 4.2
5:   end for
6:   Update_Rendering()                            ▶ subsection 4.3
7: end while

```

4.1 Hand-based User Interaction

Contact-based Modeling. To enable efficient contact handling for interactive feedback, we approximate the geometry of hands and integrated deformation tools using the medial axis transform (MAT) [Faraj et al. 2013; Stolpner et al. 2011]. The medial axis of a 3D model consists of points that are centers of maximally inscribed spheres. By incorporating radius information along the medial axis, the MAT can reconstruct the original geometry. MAT can be discretized as a small number of linearly interpolated spheres or medial primitives while precisely describing the shape. These medial primitives are classified as either medial cones or slabs [Sun et al. 2015], defined by two or three vertices on the medial axis. In our implementation, we use the quadratic error metric [Li et al. 2015] to compute the medial mesh of hands and tools. Specifically, a hand can be approximated by 76 medial cones and 28 medial slabs (Figure 3). For collision handling during simulation, we adopt the method from Medial IPC [Lan et al. 2021] to calculate distances between MPM grid nodes and medial primitives representing hands or tools. Additionally, we employ the bounding boxes of medial primitives to construct a spatial hash data structure, enabling efficient collision detection.

Beyond direct hand manipulation, we provide auxiliary modeling tools such as a planar slab, a rod, and scissors (Figure 4) to support diverse and controlled deformations, mimicking creative processes observed in the real world. Upon selection, each tool attaches to a hand joint, allowing users to control it through hand movements. Each hand operates independently, enabling seamless transitions between different tools. During hand tracking, the position and orientation of each medial primitive are determined by the nearest joints of the hand skeleton. To enhance tracking stability, we apply a moving average kernel to the data from the past 0.2 seconds, with

weights determined by frame duration. This ensures consistent and reliable hand-tracking performance across varying frame rates.

Overall, our efficient contact handling techniques enable interactive modeling operations on deformable objects, such as pinching, squeezing, and folding, while avoiding noticeable visual artifacts. We use the hand texture from Pohl and Mottelson [2022] for rendering.

Mid-air Gestural Modeling. Mid-air gestural input is advantageous when users face difficulties selecting the desired editing area on an object using contact-based modeling, which helps to avoid unintended changes to the object. We provide a mid-air pinch gesture (where the tip of the thumb touches the tip of the middle finger), enabling users to perform operations such as stretching or twisting materials by applying a force field to selected MPM particles. A green highlight is used to visualize the selection area and the applied force field, providing intuitive visual feedback. Users can further refine the radius of the selection area and adjust the force magnitude for more precise control, as shown in Figure 4.

Other Operations. Our user interface provides a range of common operations to enhance usability and ensure smooth modeling workflows. Objects in the scene can be *selected* and *moved* by grabbing their bounding boxes with the hands or by using a ray-casting gesture to intersect the bounding box. *Scaling* operations are performed by grasping the object’s bounding box with both hands and moving them outward or inward, visually scaling the object up or down without altering its physical size. This zooming functionality enables seamless transitions between fine-grained local editing and broader global shaping. To create new objects, users can *load* built-in primitive shapes, such as spheres, tori, or cubes, or utilize a *sourceing* tool that extrudes geometry with customizable cross section (e.g., circles, squares, or stars). The extrusion process dynamically samples MPM particles, with the direction and speed controlled by hand movements. Additionally, the system integrates commonly used operations in 3D modeling tools, such as *Merge*, *Copy*, *Reset*, and *Delete*, allowing users to efficiently manipulate modeled objects.

4.2 Simulation

Particle-Level Collision Handling. Due to the limited resolution of the simulation grid, MPM particles can penetrate the boundaries of

Algorithm 2 `Sim_substep()` (*More details in our supp. doc.*)

```

1: Particle_to_Grid()
2: Update_Grid_Velocity()
3: Grid_to_Particle()
4: Particle_Projection()           ▶ subsection 4.2
5: Apply_Plasticity()

```

passive objects, such as hands and tools, despite applying grid-based boundary conditions. Increasing grid resolution to fully resolve these geometries is computationally expensive and impractical. To address this issue, we introduce a particle-level collision handling step that operates independently of grid resolution.

For particles that remain inside passive objects after their states are updated using grid information in the `Grid_to_Particle` step, we project them out and adjust their velocities:

$$\mathbf{x}_p = \mathbf{x}_p + \mathbf{p}_p, \quad \text{and} \quad \mathbf{v}_p = \mathbf{v}_{\text{boundary}}, \quad (1)$$

where \mathbf{p}_p is the vector connecting the particle position \mathbf{x}_p to the closest point on the boundary, and $\mathbf{v}_{\text{boundary}}$ is the velocity of this closest point. This step ensures particles remain outside the passive objects and conform to their surface geometry, enabling accurate hand-object interactions even at moderate grid resolutions.

Localized Simulation. While MPM is effective for large deformations, real-time simulation is constrained by typical hardware capabilities, supporting approximately 100K particles. However, large-scale Gaussian splatting scenes often contain over 500K particles, making full-scene simulation infeasible in real time. To address this, we propose a localized simulation approach tailored to user interactions. Since the primary input comes from hand tracking, our system confines the simulation to a cubic region centered around the user’s hands, leaving particles outside this region stationary. This approach significantly reduces computational costs, enabling higher frame rates without compromising user experience.

4.3 Rendering

Uniform Gaussian Volume Regularization. The original 3D Gaussian Splatting (GS) method captures fine details only on the surface of objects, while the interior is typically empty or filled with a small number of large Gaussians. While this approach is sufficient for static objects, large deformations can expose the interior, leading to blurry rendering artifacts. PhysGaussian [Xie et al. 2024] attempts to address this by sampling additional Gaussians inside the object and assigning them the color of the closest surface Gaussian. However, this strategy can still result in blurry visuals in the interior during significant deformations.

To tackle this issue, we introduce a loss function during the training of 3D GS to penalize large volume differences of Gaussians:

$$L_{\text{vol_ratio}} = \max \left(\frac{\text{mean}(V_{\text{top},\alpha})}{\text{mean}(V_{\text{bottom},\alpha})}, r \right) - r, \quad (2)$$

where V represents the average volume of the top α percent of Gaussians with the largest or smallest volumes, and r is the target maximum allowable volume ratio. In practice, we find that setting $r = 2$ and $\alpha = 30\%$ yields effective results. This loss encourages Gaussians to have more uniform volumes, reducing the likelihood

of blurry artifacts and ensuring consistent visual fidelity even under large deformations.

Decoupled Appearance and Physical Representations. In Xie et al. [2024], each Gaussian is treated as an MPM particle. To accurately render complex appearances, the density of Gaussians is typically much higher than the precision required by MPM for simulating elastoplastic deformations in the context of 3D modeling. To address this mismatch, we decouple MPM particles for simulation from Gaussian kernels used for rendering. A smaller number of MPM particles drive a larger number of Gaussians through the MPM grid, maintaining rendering accuracy while significantly improving simulation efficiency. Specifically, during each simulation substep, MPM particles execute the full `Sim_Substep` first. Subsequently, Gaussian kernels use the grid velocity information from the MPM simulation to perform `Grid_to_Particle`, `Particle_Projection`, and `Apply_Plasticity`. These steps are fully parallelizable and account for only a small portion of the total computational cost in a typical MPM simulation. This decoupling strategy optimizes computational efficiency without compromising visual fidelity, ensuring a seamless balance between simulation and rendering.

Mesh Rendering. In addition to supporting the editing of 3D objects represented by Gaussian splatting, our system allows users to create models from scratch by reconstructing surface meshes from MPM particles using the Marching Cubes algorithm. Specifically, we compute the density field of the modeled objects by transferring particle mass onto a uniform grid during the `Particle_to_Grid` step and extract an isosurface to construct the mesh. This grid is independent of the simulation grid, following the decoupled appearance and physical representations. To improve surface quality, Laplacian smoothing is applied to the resulting mesh. The original Marching Cubes algorithm may create unwanted connections or "sticking" between regions of different objects that are in close proximity. To address this, a "category" attribute is assigned to each particle. During the `Particle_to_Grid` transfer, separate density fields are maintained for each particle category. The Marching Cubes algorithm is then applied independently to each density field, ensuring that each category is reconstructed as an independent mesh and rendered separately.

4.4 System Implementation

We developed our system using Unity, integrating 3D Gaussian Splatting and Marching Cubes techniques. For the simulation component, we utilized Taichi [Hu et al. 2019] as the compilation engine, which is well-suited for developing high-performance physics-based simulators. The simulation code was compiled into binary files and imported into Unity, where it was executed via C# bindings. For experiments, the system ran on a 16-core 4.3GHz AMD Ryzen 9 9950X machine with an Nvidia RTX 4090 GPU, paired with a Meta Quest 3 VR headset featuring hand-tracking functionality as the display and user input device. This setup enabled efficient and responsive interactions within the VR environment. We will open-source our code and data upon acceptance of this paper.

5 EVALUATION

In this section, we evaluate the real-time performance, visual consistency, and realism of our system, highlighting the contributions

of our technical innovations with ablation studies. Unless stated otherwise, the experimental setup is as follows: The simulation uses a grid resolution of 64^3 with 8 particles per grid cell at initialization. Each frame performs 5 simulation substeps, employing a neo-Hookean elasticity model combined with a von Mises plasticity model. For rendering, the density field is sampled at 128^3 , with mesh reconstruction via the Marching Cubes algorithm and 5 iterations of Laplacian smoothing to improve surface quality. To ensure consistent comparisons, we recorded a specific hand trajectory for each example and applied it across all tests with varying parameters.

Real-Time Performance. To evaluate the real-time performance of VR-Doh, we conducted an experiment involving a simple scenario where a sphere is compressed between two hands (as shown in Figure 5, bottom row). To analyze performance scalability, we varied the simulation grid resolution, the number of substeps per frame, and the number of particles per grid cell, while keeping other parameters constant. The overall FPS under these conditions is summarized in Figure 9. The results demonstrate that VR-Doh can maintain real-time performance, achieving interactive frame rates even with higher computational demands, such as a 100^3 simulation grid resolution, 30 substeps per frame, and 12 particles per cell.

Convergence Under Spatial Refinement. To validate the consistency of our simulation, we conducted an experiment where a hand trajectory presses into a sphere to create a hole and then squeezes it from both sides. The simulation was tested with varying grid resolutions while keeping the number of particles per cell constant. As shown in Figure 10, the deformations converge once the grid resolution exceeds 48^3 , indicating that our simulation achieves consistent and accurate results without requiring excessively high resolutions.

Particle-Level Collision Handling. In Figure 5, we compare the traditional MPM boundary condition with and without our particle-level collision handling using a hand imprint (top row) and a sphere compression (bottom row) example. As shown in the figure, applying particle-level collision handling produces significantly clearer imprints, enhancing the ability to adjust finer details. However, the results in the second row demonstrate that using only particle-level collision handling can lead to severe volume loss, as the particle projection step does not account for elastoplasticity forces. By combining both methods, our approach achieves realistic overall deformations while enabling precise adjustments for detailed modeling.

Table 1. **Localized Simulation.** Comparison of FPS with and without localized simulation in large 3D Gaussian Splatting scenes, showing an average frame rate improvement of 3.3× with localized simulation enabled.

Scene	Splats count	FPS w/o localized sim.	FPS w localized sim.
Garden	660K	12.2	39.8
Bicycle	480K	13.1	43.5
Room	382K	13.6	44.5

Localized Simulation. We evaluated VR-Doh’s performance with and without localized simulation across several typical 3D GS scenes, including Garden, Bicycle, and Room, each containing several hundred thousand Gaussians. During the tests, users navigated through each scene and interacted with primary objects using hand gestures, introducing deformations. As shown in Table 1, enabling localized

simulation resulted in an average frame rate improvement of 3.3×, demonstrating its significant impact on performance.

Uniform Gaussian Volume Regularizer. We evaluated the effectiveness of our Uniform Gaussian Volume Regularization by simulating a textured sand cube represented with 3D Gaussians as it was dropped onto the ground under gravity, resulting in significant deformations. Figure 6 compares the original model (left) with the deformed results using (middle) and without (right) the proposed volume regularization loss. Without the loss, the exposed interior reveals noticeable blurry artifacts caused by uneven Gaussian volumes. In contrast, applying the regularization maintains consistent Gaussian volumes, preserving sharp details and achieving high visual fidelity even under extreme deformation.

Decoupled Appearance and Physical Representations. We evaluated the performance of our method under different sampling ratios between MPM particles and Gaussian kernels in a simulation where a wolf sits on the ground under gravity. Here, we maintain the MPM particle per cell, so the simulation grid resolution decreases as we downsample MPM particles. Figure 7 illustrates the original (left) and deformed (right) configurations and the FPS achieved with varying sampling ratios. The results show that as the sampling ratio decreases—fewer MPM particles driving the 3D Gaussians—the wolf’s volume slightly increases while maintaining high visual fidelity and preserving detailed features. This behavior is expected, as lower resolutions in MPM typically exhibit stiffer deformation due to discretization errors. Notably, by reducing MPM particles to approximately 30% of the Gaussian kernels, the FPS nearly doubles, demonstrating the effectiveness of our approach to decouple appearance and physical representations, achieving significant performance gains without sacrificing visual quality.

6 CASE STUDY

Featured Operations. Figure 4 highlights featured modeling operations in VR-Doh, including contact-based shape editing with hands and tools like slabs and rods, mid-air gesture-based bending and twisting, and the sourcing tool for adding new materials. The objects exhibit realistic elastoplastic deformations, closely resembling real-world behavior. This physical realism enables users to intuitively model objects by drawing on their real-life experiences.

Object Creation. We demonstrate object creation using VR-Doh, as shown in Figure 8. In the first row, a snowman is assembled, starting with a blank snowfield, molding the body, and adding details. The second row demonstrates the creation of a hamburger by stacking individual components to form a layered structure. In the third row, a panda is carefully modeled from head to body, incorporating bamboo as an accessory that seamlessly integrates with its hands. The fourth row depicts the crafting of a Swiss roll, where layers are rolled together to replicate a realistic pattern. Finally, the fifth row shows the formation of steamed buns, shaped and arranged within a bamboo steamer. These examples highlight VR-Doh’s strength in simplifying tasks that require precise spatial arrangements, which are significantly more challenging to achieve using a mouse on a 2D screen. With VR-Doh, object creation becomes as natural and intuitive as manipulating items in the real world.

3D GS Object Editing. Figure 11 demonstrates 8 examples of editing GS-represented objects, showcasing the intuitive and creative capabilities of VR-Doh. First, multiple mushroom-shaped houses were assembled, with their roofs sharpened and the mushrooms enlarged through hand manipulation and mid-air pinch gestures. The text "VR-Doh" was then sculpted onto the roof by hand. Next, a red pig transitioned from running to performing ballet through flexible selection and dragging of specific body parts, with its head rotated to face the audience using the pinch gesture. Two statues were brought to 'life': a terracotta figurine joyfully lifted its head and began drumming, while the Discobolus threw its discus with dynamic force. This involved using hands to cut and separate the discus before repositioning it. Moving on, wooden frames were interlocked and freely stacked into an arch through gravity and contact interactions, then merged seamlessly with greenery. The greenery's complex shapes were also easily refined by hand. A girl's posture was adjusted as her arms bent to mimic the act of eating a watermelon. Following that, flowers on a vase were flexibly selected using the pinch gesture, then intertwined in space with penetrations automatically avoided, demonstrating precise and convenient control. Finally, a capybara plush toy was made to appear fatter, while its head decoration was reshaped into a strawberry and placed in the front. These examples highlight VR-Doh's ability to simplify complex modeling tasks while maintaining creativity and controllability. All examples are available on an anonymous online [3D viewer](#).

7 USER STUDY

To evaluate VR-Doh's usability, effectiveness, and potential applications, we conducted two user studies involving both novice and expert participants. The first study (*US1*) focused on open-ended creative tasks to assess the system's intuitiveness, immersion, and efficiency in 3D modeling. The second study (*US2*) directly compared VR-Doh with the conventional modeling software Blender, highlighting their respective strengths and limitations. We briefly summarize the process and findings of the two user studies here, with detailed information provided in the supplemental document.

US1: Usability and Effectiveness of VR-Doh. US1 involved 12 participants, including 6 experts (P1-P6) with 3-5 years of 3D modeling experience and 6 novices (P7-P12) without prior experience, to evaluate VR-Doh's usability and performance. Participants were tasked with (1) editing a pre-existing 3D model (e.g., reshaping a plush toy) and (2) creating a 3D model from scratch (e.g., designing a snowman). After practicing basic operations, participants performed these tasks and completed the USE questionnaire [Lund 2001] to evaluate usability and the Simulator Sickness Questionnaire (SSQ) [Kennedy et al. 1993] to assess discomfort. A 10-minute semi-structured interview was also conducted to gather detailed feedback.

Both expert and novice participants found VR-Doh intuitive, immersive, and efficient, with design outcomes closely matching their expectations (Figure 12). The system received high ratings for usefulness (5.6/7), ease of use (5.5/7), ease of learning (6.0/7), and satisfaction (5.9/7), with no reports of discomfort or nausea. Participants praised the natural interaction modes, such as hand manipulation and mid-air gestures, for enabling realistic deformation and intuitive viewpoint control. Features like switching material types, leveraging gravity for stacking, and real-time rendering were particularly

appreciated. However, limitations such as hand-tracking instability and the lack of an undo feature were noted, alongside suggestions for improved precision.

US2: Comparison with Blender. US2 compared VR-Doh with conventional desktop-based modeling software, specifically Blender 4.3, involving six participants (four with 3-7 years of modeling experience and two without). Participants performed two goal-directed tasks—creating a Swiss roll and a donut—using both tools, guided by a step-by-step video tutorial. The order of tools was counterbalanced to minimize learning effects. On average, participants completed both tasks faster using VR-Doh and expressed a preference for its intuitive and natural interaction, particularly for the Swiss roll task.

Four key advantages of VR-Doh were identified: (1) flexible selection through dexterous hand movements, enabling "what-you-see-is-what-you-get" precision and avoiding over-/under-selection issues common in 2D-projected views; (2) realistic deformation leveraging elastoplastic simulation for intuitive editing of shapes and materials; (3) pose editing without rigging, where body parts can be adjusted directly with smooth joint transitions enabled by simulation; and (4) physics-based cutting, allowing objects to be physically separated at weak points without sophisticated manual adjustments of cutting planes. Participants found VR-Doh particularly effective for quickly shaping overall structures and realizing design ideas, although its precision in specialized tasks was lower than Blender due to real-time simulation constraints and the lack of haptic feedback. Overall, VR-Doh and Blender exhibited complementary strengths, with VR-Doh excelling in intuitive, global operations and Blender providing superior precision for detailed edits.

8 CONCLUSION

We presented VR-Doh, a VR-based 3D modeling system that integrates advanced elastoplastic simulation with intuitive, hand-based interaction. Leveraging the Material Point Method (MPM) and incorporating innovations such as localized simulation, particle-level collision handling, and decoupled appearance and physical representations, the system achieves real-time responsiveness while delivering high-quality simulation and rendering. These technical innovations make VR-Doh accessible to novice users while empowering experts to perform detailed and expressive modeling. Extensive evaluations and user studies showcased the system's ability to provide an intuitive and immersive modeling experience. Compared to traditional tools, VR-Doh offers a more natural and accessible approach, with user-identified advantages such as flexible selection, realistic deformation, rig-free pose editing, and physics-based cutting, paving the way for a new paradigm in 3D modeling.

Discussion and Future Works. Our method offers several promising directions for future research. Unlike traditional modeling software, where operations are typically localized or abstracted, allowing for straightforward undo functionality, our simulation-based tool modifies the entire domain with each operation. Even slight variations in input trajectories can produce significantly different outcomes. While our current solution relies on periodically saving states, developing a memory-efficient undo mechanism would be highly beneficial. Additionally, the absence of haptic feedback in our system makes it challenging for users to avoid unintended modifications,

especially in occluded regions. Improving the user experience could involve incorporating advanced haptic devices or exploring alternative feedback mechanisms, such as auditory cues, while ensuring accessibility remains a priority.

REFERENCES

2025. *GravitySketch*. <https://gravitysketch.com/>
2025. *Shapelab*. <https://shapelabvr.com/>
- Rahul Arora, Rubaiat Habib Kazi, Danny M Kaufman, Wilmot Li, and Karan Singh. 2019. Magicalhands: Mid-air hand gestures for animating in vr. In *Proceedings of the 32nd annual ACM symposium on user interface software and technology*. 463–477.
- Héctor Barreiro, Joan Torres, and Miguel A Otaduy. 2021. Natural tactile interaction with virtual clay. In *2021 IEEE World Haptics Conference (WHC)*. IEEE, 403–408.
- Shounak Chatterjee. 2024. Free-form Shape Modeling in XR: A Systematic Review. *arXiv preprint arXiv:2401.00924* (2024).
- Hanchen Deng, Jin Li, Yang Gao, Xiaohui Liang, Hongyu Wu, and Aimin Hao. 2023. PhyVR: Physics-based Multi-material and Free-hand Interaction in VR. In *2023 IEEE International Symposium on Mixed and Augmented Reality (ISMAR)*. IEEE, 454–462.
- Guillaume Dewaele and Marie-Paule Cani. 2004. Interactive global and local deformations for virtual clay. *Graphical Models* 66, 6 (2004), 352–369.
- Sevinc Eroglu, Sascha Gebhardt, Patric Schmitz, Dominik Rausch, and Torsten Wolfgang Kuhlén. 2018. Fluid sketching—Immersive sketching based on fluid flow. In *2018 IEEE Conference on Virtual Reality and 3D User Interfaces (VR)*. IEEE, 475–482.
- Yu Fang, Minchen Li, Chenfanfu Jiang, and Danny M. Kaufman. 2021. Guaranteed Globally Injective 3D Deformation Processing. *ACM Trans. Graph. (SIGGRAPH)* 40, 4, Article 75 (2021).
- Noura Faraj, Jean-Marc Thiery, and Tamy Boubekeur. 2013. Progressive medial axis filtration. In *SIGGRAPH Asia 2013 Technical Briefs*. 1–4.
- Markus Höll, Markus Oberweger, Clemens Arth, and Vincent Lepetit. 2018. Efficient physics-based implementation for realistic hand-object interaction in virtual reality. In *2018 IEEE conference on virtual reality and 3D user interfaces (VR)*. IEEE, 175–182.
- Yuanming Hu, Yu Fang, Ziheng Ge, Ziyin Qu, Yixin Zhu, Andre Pradhana, and Chenfanfu Jiang. 2018. A moving least squares material point method with displacement discontinuity and two-way rigid body coupling. *ACM Transactions on Graphics (TOG)* 37, 4 (2018), 1–14.
- Yuanming Hu, Tzu-Mao Li, Luke Anderson, Jonathan Ragan-Kelley, and Frédo Durand. 2019. Taichi: a language for high-performance computation on spatially sparse data structures. *ACM Transactions on Graphics (TOG)* 38, 6 (2019), 1–16.
- Jan Jacobs and Bernd Froehlich. 2011. A soft hand model for physically-based manipulation of virtual objects. In *2011 IEEE virtual reality conference*. IEEE, 11–18.
- Chenfanfu Jiang, Craig Schroeder, Joseph Teran, Alexey Stomakhin, and Andrew Selle. 2016. The material point method for simulating continuum materials. In *Acm siggraph 2016 courses*. 1–52.
- Ying Jiang, Chang Yu, Tianyi Xie, Xuan Li, Yutao Feng, Huamin Wang, Minchen Li, Henry Lau, Feng Gao, Yin Yang, et al. 2024. VR-GS: a physical dynamics-aware interactive gaussian splatting system in virtual reality. In *ACM SIGGRAPH 2024 Conference Papers*. 1–1.
- Robert S Kennedy, Norman E Lane, Kevin S Berbaum, and Michael G Lilienthal. 1993. Simulator sickness questionnaire: An enhanced method for quantifying simulator sickness. *The international journal of aviation psychology* 3, 3 (1993), 203–220.
- Bernhard Kerbl, Georgios Kopanas, Thomas Leimkühler, and George Drettakis. 2023. 3D Gaussian Splatting for Real-Time Radiance Field Rendering. *ACM Trans. Graph.* 42, 4 (2023), 139–1.
- Vikash Kumar and Emanuel Todorov. 2015. Mujoco haptix: A virtual reality system for hand manipulation. In *2015 IEEE-RAS 15th International Conference on Humanoid Robots (Humanoids)*. IEEE, 657–663.
- Lei Lan, Yin Yang, Danny Kaufman, Junfeng Yao, Minchen Li, and Chenfanfu Jiang. 2021. Medial IPC: accelerated incremental potential contact with medial elastics. *ACM Transactions on Graphics* 40, 4 (2021).
- Pan Li, Bin Wang, Feng Sun, Xiaohu Guo, Caiming Zhang, and Wenping Wang. 2015. Q-mat: Computing medial axis transform by quadratic error minimization. *ACM Transactions on Graphics (TOG)* 35, 1 (2015), 1–16.
- Christos Lougiakis, Jorge Juan González, Giorgos Ganiás, Akrivi Katifori, Maria Roussou, et al. 2024. Comparing Physics-based Hand Interaction in Virtual Reality: Custom Soft Body Simulation vs. Off-the-Shelf Integrated Solution. In *2024 IEEE Conference Virtual Reality and 3D User Interfaces (VR)*. IEEE, 743–753.
- Arnold M Lund. 2001. Measuring usability with the use questionnaire12. *Usability interface* 8, 2 (2001), 3–6.
- Michael R Marner and Bruce H Thomas. 2010. Augmented foam sculpting for capturing 3D models. In *2010 IEEE Symposium on 3D User Interfaces (3DUI)*. IEEE, 63–70.
- Kevin T McDonnell, Hong Qin, and Robert A Wlodarczyk. 2001. Virtual clay: A real-time sculpting system with haptic toolkits. In *Proceedings of the 2001 symposium on Interactive 3D graphics*. 179–190.
- Joss Kingdom Moo-Young, Andrew Hogue, and Veronika Szkudlarek. 2021. Virtual materiality: Realistic clay sculpting in vr. In *Extended Abstracts of the 2021 Annual Symposium on Computer-Human Interaction in Play*. 105–110.
- Andrew Nealen, Takeo Igarashi, Olga Sorkine, and Marc Alexa. 2007. Fibermesh: designing freeform surfaces with 3d curves. In *ACM SIGGRAPH 2007 papers*. 41–es.
- Adeline Pihuit, Paul G Kry, and Marie-Paule Cani. 2008. Hands on virtual clay. In *2008 IEEE International Conference on Shape Modeling and Applications*. IEEE, 267–268.
- Henning Pohl and Aske Mottelson. 2022. Hafnia Hands: A Multi-Skin Hand Texture Resource for Virtual Reality Research. *Frontiers in Virtual Reality* 3 (2022).
- Enrique Rosales, Chrystiano Araújo, Jafet Rodriguez, Nicholas Vining, Dongwook Yoon, and Alla Sheffer. 2021. AdaptiBrush: adaptive general and predictable VR ribbon brush. *ACM Trans. Graph.* 40, 6 (2021), 247–1.
- Enrique Rosales, Jafet Rodriguez, and Alla Sheffer. 2019. SurfaceBrush: from virtual reality drawings to manifold surfaces. *arXiv preprint arXiv:1904.12297* (2019).
- Steven Schkolne, Michael Pruett, and Peter Schröder. 2001. Surface drawing: creating organic 3D shapes with the hand and tangible tools. In *Proceedings of the SIGCHI conference on Human factors in computing systems*. 261–268.
- HJ Schulz, M Teschner, and M Wimmer. 2019. Rodmesh: Two-handed 3D surface modeling in virtual reality. In *Vision, modeling and visualization*. 1–10.
- Jia Sheng, Ravin Balakrishnan, and Karan Singh. 2006. An interface for virtual 3D sculpting via physical proxy. In *GRAPHITE*, Vol. 6. 213–220.
- Breannan Smith, Chenglei Wu, He Wen, Patrick Peluse, Yaser Sheikh, Jessica K Hodgins, and Takaaki Shiratori. 2020. Constraining dense hand surface tracking with elasticity. *ACM Transactions on Graphics (ToG)* 39, 6 (2020), 1–14.
- Svetlana Stolpner, Paul Kry, and Kaleem Siddiqi. 2011. Medial spheres for shape approximation. *IEEE transactions on pattern analysis and machine intelligence* 34, 6 (2011), 1234–1240.
- Feng Sun, Yi-King Choi, Yizhou Yu, and Wenping Wang. 2015. Medial meshes—a compact and accurate representation of medial axis transform. *IEEE transactions on visualization and computer graphics* 22, 3 (2015), 1278–1290.
- Mickeal Verschoor, Daniel Lobo, and Miguel A Otaduy. 2018. Soft hand simulation for smooth and robust natural interaction. In *2018 IEEE conference on virtual reality and 3D user interfaces (VR)*. IEEE, 183–190.
- Tianyi Xie, Zeshun Zong, Yuxing Qiu, Xuan Li, Yutao Feng, Yin Yang, and Chenfanfu Jiang. 2024. Physgaussian: Physics-integrated 3d gaussians for generative dynamics. In *Proceedings of the IEEE/CVF Conference on Computer Vision and Pattern Recognition*. 4389–4398.
- Emilie Yu, Rahul Arora, Tibor Stanko, J Andreas Bærentzen, Karan Singh, and Adrien Bousseau. 2021. Cassie: Curve and surface sketching in immersive environments. In *Proceedings of the 2021 CHI Conference on Human Factors in Computing Systems*. 1–14.

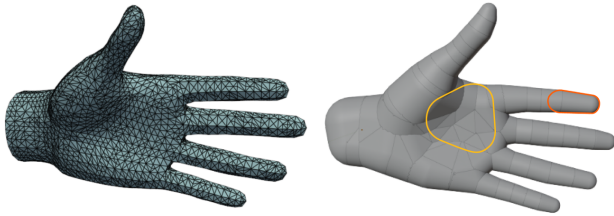


Fig. 3. **Medial axis approximation of hand geometry.** The highlighted curves indicate the boundaries of a specific medial slab and a medial cone.

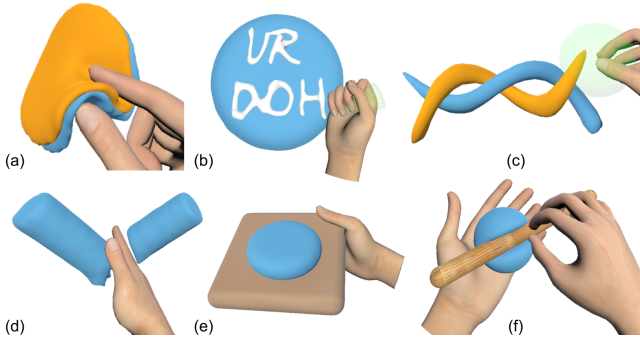


Fig. 4. **Featured Operations:** (a) Pinching and reshaping with fingers; (b) Using a sourcing tool to extrude new materials onto an object; (c) Mid-air gestures for bending and twisting objects; (d) Hand-based cutting of objects; (e) Tool-based operations with a slab and a rod.

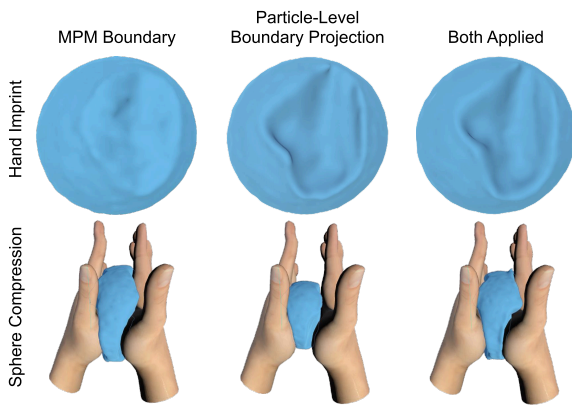


Fig. 5. **Particle-Level Collision Handling.** Comparison of MPM boundary conditions with and without particle-level collision handling on a hand imprint (top) and a sphere compression (bottom) example. Combining both methods (right) achieves realistic deformations with enhanced detail while avoiding volume loss.

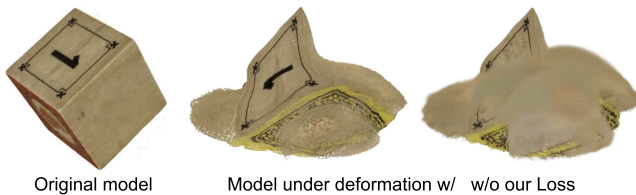


Fig. 6. **Uniform Gaussian Volume Regularizer.** Comparison of a sand cube dropped under gravity shows that applying the regularization (middle) preserves sharp details and avoids blurry artifacts in the interior (right), ensuring high visual fidelity during large deformations.

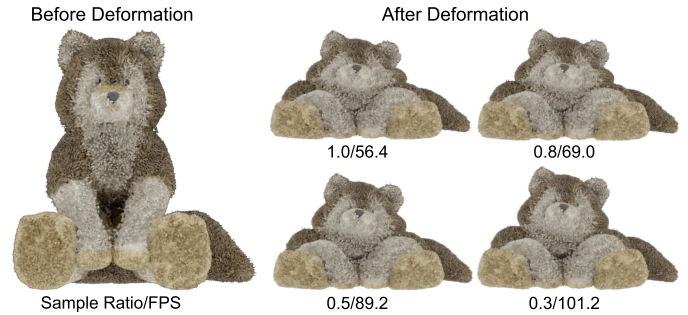


Fig. 7. **Decoupled Appearance and Physical Representations.** This example of a wolf sitting under gravity demonstrates that reducing the number of MPM particles driving the 3D Gaussians slightly increases the wolf’s volume but maintains high visual fidelity while significantly improving FPS, showcasing the effectiveness of our approach.



Fig. 8. **Object Creation Examples.** Crafting a snowman, assembling a hamburger with gravity-stacked layers, creating a panda holding bamboo, rolling a Swiss roll, and shaping steamed buns in a bamboo steamer, showcasing intuitive and precise 3D modeling. More examples are available on an anonymous online [3D viewer](#).

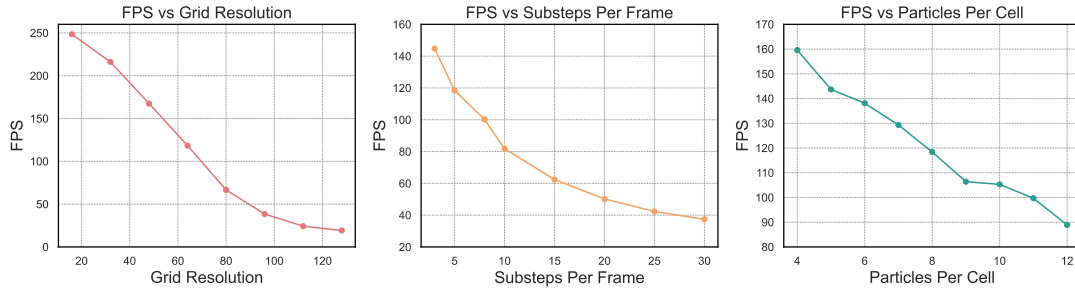


Fig. 9. **Real-Time Performance Evaluation.** FPS of VR-Doh with varying simulation grid resolution, substeps per frame, and MPM particles per cell in a sphere compression scenario (Figure 5, bottom). Results demonstrate VR-Doh’s ability to maintain real-time performance under high computational demands.

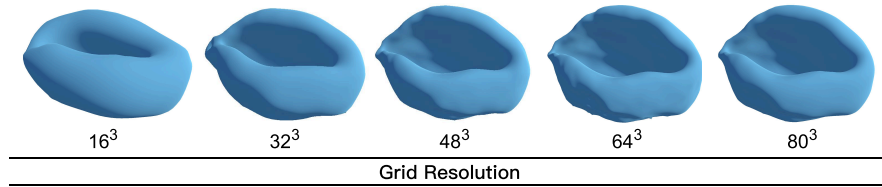


Fig. 10. **Convergence under Spatial Refinement.** Sphere deformations under identical hand imprints and squeezing converge at resolutions above 48^3 , ensuring accuracy without excessive computational cost.



Fig. 11. **3D GS object editing examples.** Users combined, reshaped, and customized models using hand gestures and tools, bringing objects to life, merging elements seamlessly, and refining intricate details with ease. These examples highlight VR-Doh’s ability to simplify complex modeling tasks while preserving creativity and control. More examples are available on an anonymous online 3D viewer.



Fig. 12. **User Study Outcomes.** Edited 3D GS models (top row) and newly created models (bottom row) by novice and expert participants.

VR-Doh: Hands-on 3D Modeling in Virtual Reality

Supplemental Document

ZHAOFENG LUO*, Carnegie Mellon University, USA and Peking University, China
ZHITONG CUI*, Carnegie Mellon University, USA and Zhejiang University, China
SHIJIAN LUO, Zhejiang University, China
MENGYU CHU, Peking University, China
MINCHEN LI, Carnegie Mellon University, USA

CCS Concepts: • **Computing methodologies** → **Virtual reality**; *Point-based models*.

Additional Key Words and Phrases: Virtual Reality, Human-Computer Interactions, 3D Modeling, Elastoplasticity Simulator, Material Point Method

CONTENTS

Contents	1
1 Technical Background	1
1.1 MLS-MPM	1
1.2 PhysGaussian	3
2 Technical Details of MLS-MPM	3
2.1 First Piola-Kirchoff Stress	3
2.2 Plasticity	4
3 User Study 1: Usability and Effectiveness of VR-Doh	5
3.1 Semi-Structured Interview Results (Experts, P1-P6)	5
3.2 Semi-Structured Interview Results (Novices, P7-P12)	7
4 User Study 2: Comparison with Blender	7
4.1 Semi-Structured Interview Results	8
References	8

1 TECHNICAL BACKGROUND

Based on our design rationale, we selected PhysGaussian [Xie et al. 2024] as the foundation of our system to enable real-time simulation of elastoplastic objects and achieve photorealistic rendering. This section provides a technical background on the Moving Least Squares (MLS) Material Point Method (MPM) [Hu et al. 2018] and 3D Gaussian Splatting [Kerbl et al. 2023], which PhysGaussian builds upon.

1.1 MLS-MPM

The Moving Least Squares Material Point Method (MLS-MPM) [Hu et al. 2018] is a hybrid Lagrangian-Eulerian approach well suited for simulating multi-material phenomena. In this framework, Lagrangian particles track

*Both authors contributed equally to this research.

Authors' Contact Information: Zhaofeng Luo, Carnegie Mellon University, USA and Peking University, China, roushelfy@stu.pku.edu.cn; Zhitong Cui, Carnegie Mellon University, USA and Zhejiang University, China, zhitongcui@zju.edu.cn; Shijian Luo, Zhejiang University, China, sjluo@zju.edu.cn; Mengyu Chu, Peking University, China, mchu@pku.edu.cn; Minchen Li, Carnegie Mellon University, USA, minchernl@gmail.com.

Algorithm 1 Sim_substep()

-
- 1: Particle_to_Grid()
 - 2: Update_Grid_Velocity()
 - 3: Grid_to_Particle()
 - 4: Particle_Projection() ▷ Main Paper
 - 5: Apply_Plasticity()
-

the geometry and material properties of the simulated object, while a Eulerian background grid facilitates force computation and time integration. This dual representation enables MPM to efficiently handle large deformations, topology changes, and contact by transferring physical quantities, such as mass and momentum, between particles and the grid, leveraging the strengths of each spatial discretization [Jiang et al. 2016; Sulsky et al. 1995].

Each MPM simulation time step (Algorithm 1) begins with the `Particle_to_Grid` operation, transferring particle mass and momentum to neighboring grid nodes:

$$\begin{aligned}
 m_i^n &= \sum_p w_{i,p}^n m_p, \\
 m_i^n \mathbf{v}_i^n &= \sum_p w_{i,p}^n (m_p \mathbf{v}_p + (m_p \mathbf{C}_p^n - \mathbf{E}_p^n)(\mathbf{x}_i - \mathbf{x}_p^n)).
 \end{aligned} \tag{1}$$

Here, subscripts p and i correspond to particle and grid quantities, respectively, while the superscript indicates the time step. m is the mass, and w is the weight for the transfer, which is nonzero only for particles and grid nodes that are close. \mathbf{v} is the velocity, \mathbf{x} is the position, \mathbf{C}_p stores information about the local velocity field around particle p , and $\mathbf{E}_p^n = -\frac{4\Delta t}{\Delta x^2} \sum_p V_p^0 \mathbf{P}_p^n (\mathbf{F}_p^n)^T$ is the elasticity stress term. Here, Δt is the time step size, Δx is the grid spacing, V_p^0 is the initial volume of particle p , \mathbf{F} is the deformation gradient, and \mathbf{P} is the first Piola-Kirchhoff stress calculated using \mathbf{F} .

In the `Update_Grid_Velocity` step, grid velocities are updated to incorporate external forces \mathbf{f}_{ext} , such as gravity and air damping:

$$\hat{\mathbf{v}}_i^n = \mathbf{v}_i^n + \frac{1}{m_i^n} \mathbf{f}_{ext,i}^n \cdot \Delta t. \tag{2}$$

To handle simulation domain boundaries and forces from passive objects, such as tracked human hands, *slip* or *sticky* boundary conditions are enforced. For slip boundaries, the normal component of the relative velocity near the boundary is set to zero, while for sticky boundaries, both tangential and normal components are set to zero to simulate friction.

Following this, the `Grid_to_Particle` operation updates particle states based on nearby grid nodes:

$$\begin{aligned}
 \mathbf{v}_p^{n+1} &= \sum_p w_{i,p}^n \hat{\mathbf{v}}_i^n, & \mathbf{x}_p^{n+1} &= \mathbf{x}_p^n + \Delta t \hat{\mathbf{v}}_i^n, \\
 \mathbf{C}_p^{n+1} &= \frac{\Delta t}{\Delta x^2} \sum_p w_{i,p}^n \hat{\mathbf{v}}_i^n (\mathbf{x}_i - \mathbf{x}_p^n)^T, & \mathbf{F}_p^{n+1} &= (\mathbf{I} + \Delta t \mathbf{C}_p^n) \mathbf{F}_p^n.
 \end{aligned} \tag{3}$$

Since boundary conditions are enforced at the grid level, particles may still penetrate solid boundaries, especially for fine geometries not adequately resolved by the grid. To address this, our system introduces a particle-level collision handling via an additional `Particle_Projection` step, ensuring more accurate handling of particle-boundary interactions (details in the main paper).

Finally, the `Apply_Plasticity` step updates the deformation gradient \mathbf{F}_p^{n+1} through the return mapping function $Z(\cdot)$, which projects stresses outside the elastic zone back onto the yield surface of elastoplastic materials. The resulting change in \mathbf{F}_p^{n+1} represents permanent plastic deformations that are not recovered by elastic forces. Further details are provided in the supplemental document.

1.2 PhysGaussian

3D Gaussian Splatting (GS) [Kerbl et al. 2023] employs a set of unstructured 3D Gaussian kernels to efficiently represent and render a scene. Each Gaussian kernel is characterized by its center \mathbf{x}_k , covariance matrix \mathbf{A}_k , and density function:

$$G_k(\mathbf{x}) = e^{-\frac{1}{2}(\mathbf{x}-\mathbf{x}_k)^T \mathbf{A}_k^{-1}(\mathbf{x}-\mathbf{x}_k)}, \quad (4)$$

opacity σ_k , and spherical harmonic coefficients C_k . Unlike neural radiation fields (NeRFs) [Mildenhall et al. 2021], which represent scenes using neural implicit functions and render views by casting camera rays, GS directly projects 3D Gaussians onto a 2D image plane, enabling highly efficient rendering and training. Additionally, the explicit representation of 3D GS facilitates convenient scene editing, as demonstrated in works such as Chen et al. [2024]; Gao et al. [2024].

During rendering, the final color C of each pixel is computed as a weighted sum of the projected Gaussian kernels' colors:

$$C = \sum_{k \in P} \alpha_k SH(\mathbf{d}_k; C_k) \prod_{j=1}^{k-1} (1 - \alpha_j), \quad (5)$$

where P is the set of all Gaussians contributing to the pixel color, ordered by view depth; α_k is the effective opacity, calculated as the product of σ_k and the density projected onto the pixel; SH represents the spherical harmonic function; and \mathbf{d}_k is the view direction.

While GS primarily focuses on visual appearance, it does not incorporate physical properties. PhysGaussian [Xie et al. 2024] extends GS by integrating MPM, treating each Gaussian kernel as a Lagrangian particle to track displacement and deformation. This enables the simulation of elastoplastic behaviors under external forces or boundary conditions, creating a unified simulation-rendering framework. In PhysGaussian, at time t , the density of a deformed Gaussian k is calculated as:

$$G_k(\mathbf{x}, t) = e^{-\frac{1}{2}(\mathbf{x}-\mathbf{x}_k(t))^T (\mathbf{F}_k(t) \mathbf{A}_k \mathbf{F}_k(t)^T)^{-1} (\mathbf{x}-\mathbf{x}_k(t))}, \quad (6)$$

where $\mathbf{x}_k(t)$ and $\mathbf{F}_k(t)$ are the current position and deformation gradient, respectively, of the corresponding MPM particle, provided by the simulation.

We observed that properly simulating the deformation and dynamics of elastoplastic materials for geometric modeling often requires significantly fewer degrees of freedom (DOFs) than rendering their complex appearance. To address this, we customized the framework by decoupling the appearance and physical representations, allowing fewer MPM particles than Gaussian kernels, thereby enabling real-time simulation. See our main paper for more details.

2 TECHNICAL DETAILS OF MLS-MPM

2.1 First Piola-Kirchoff Stress

To calculate the first Piola-Kirchoff stress \mathbf{P}_p^n , two forms are available: StVK and neo-Hookean, defined respectively as:

$$\mathbf{P}_p^n = 2\mu \left(\mathbf{F}_p^n - \mathbf{U}\mathbf{V} \right) + \lambda \left(J_p^n - 1 \right) J_p^n \left(\mathbf{F}_p^n \right)^{-T}, \quad (7)$$

$$\mathbf{P}_p^n = \mu \left(\mathbf{F}_p^n \cdot \mathbf{F}_p^{nT} \right) + \mathbf{I} \cdot \left(\lambda \log(J) - \mu \right). \quad (8)$$

Here, μ and λ are the Lamé constants, representing the shear stiffness and incompressibility of the material, and $J = \det(\mathbf{F})$, measuring local volume change. The terms \mathbf{V} and \mathbf{U} are obtained through singular value decomposition of the deformation gradient tensor: $\mathbf{F} = \mathbf{U}\Sigma\mathbf{V}$.

2.2 Plasticity

Three types of plasticity models are often applied: Drucker-Prager, von Mises, and clamp-based plasticity. Here, we first provide the return mapping functions $Z(\cdot)$ of each plasticity model, and then explain all the symbols in the equation.

For Drucker-Prager plasticity:

$$Z(\mathbf{F}_p)_{drucker} = \begin{cases} \mathbf{F}_p, & \delta\gamma \leq 0 \\ \mathbf{U} \exp\left(\boldsymbol{\epsilon} - \delta\gamma \frac{\hat{\boldsymbol{\epsilon}}}{\|\hat{\boldsymbol{\epsilon}}\|}\right) \mathbf{V}^T, & \text{otherwise} \end{cases} \quad (9)$$

with

$$\delta\gamma = \begin{cases} \|\hat{\boldsymbol{\epsilon}}\|, & \text{tr}(\boldsymbol{\epsilon}) > 0 \\ \|\hat{\boldsymbol{\epsilon}}\| + \alpha \frac{d\lambda + 2\mu}{2\mu} \text{tr}(\boldsymbol{\epsilon}), & \text{otherwise} \end{cases} \quad (10)$$

For Von Mises plasticity:

$$Z(\mathbf{F}_p)_{von} = \begin{cases} \mathbf{F}_p, & \delta\gamma \leq 0 \\ \mathbf{U} \exp\left(\boldsymbol{\epsilon} - \delta\gamma \frac{\hat{\boldsymbol{\epsilon}}}{\|\hat{\boldsymbol{\epsilon}}\|}\right) \mathbf{V}^T, & \text{otherwise} \end{cases} \quad (11)$$

where

$$\delta\gamma = \|\hat{\boldsymbol{\epsilon}}\| - \frac{\tau_Y}{2\mu} \quad (12)$$

Clamp-based plasticity is defined as:

$$Z(\mathbf{F}_p)_{clamp} = \mathbf{U} \cdot \text{Clamp}(\Sigma, \Sigma_{\min}, \Sigma_{\max}) \cdot \mathbf{V}^T. \quad (13)$$

Explanation of Symbols.

- \mathbf{F}_p : Plastic deformation gradient tensor, representing the irreversible plastic component of the deformation.
- $Z(\mathbf{F}_p)$: Updated plastic deformation gradient after applying the plasticity return mapping. Subscripts (e.g., "drucker", "von", or "clamp") specify the model being applied (Drucker-Prager, Von Mises, or Clamp-based).
- $\mathbf{U}, \Sigma, \mathbf{V}$: Components from the Singular Value Decomposition (SVD) of the deformation gradient $\mathbf{F}_p = \mathbf{U}\Sigma\mathbf{V}^T$, where:
 - \mathbf{U} : Left singular vectors (orthogonal matrix).
 - Σ : Diagonal matrix of singular values, representing principal stretches.
 - \mathbf{V}^T : Transposed right singular vectors (orthogonal matrix).
- $\boldsymbol{\epsilon} = \log(\Sigma^{\text{tr}})$: Hencky strain tensor, computed as the logarithm of the trial singular values Σ^{tr} .
- $\hat{\boldsymbol{\epsilon}}$: Deviatoric part of the Hencky strain tensor, removing the volumetric component:

$$\hat{\boldsymbol{\epsilon}} = \boldsymbol{\epsilon} - \frac{1}{3} \text{tr}(\boldsymbol{\epsilon}) \mathbf{I},$$

where \mathbf{I} is the identity matrix.

- $\|\hat{\boldsymbol{\epsilon}}\|$: Frobenius norm of the deviatoric Hencky strain tensor, representing its magnitude.
- $\delta\gamma$: Plastic multiplier, indicating the magnitude of plastic flow during the return mapping.
- $\text{tr}(\boldsymbol{\epsilon})$: Trace of the Hencky strain tensor, representing the volumetric strain.
- α : Material parameter in the Drucker-Prager model, related to the friction angle and material properties.
- μ : Shear modulus, a material constant characterizing resistance to shear deformation.

- λ : First Lamé parameter, characterizing resistance to volumetric deformation.
- τ_Y : Yield stress in shear, a material parameter for Von Mises plasticity.
- $d\lambda$: Material-dependent parameter, often related to elastic properties such as the bulk modulus.
- $\Sigma_{\min}, \Sigma_{\max}$: Minimum and maximum limits for singular values in Clamp-based plasticity.
- $\text{Clamp}(\Sigma, \Sigma_{\min}, \Sigma_{\max})$: Function that clamps the singular values of Σ to lie within the range $[\Sigma_{\min}, \Sigma_{\max}]$.

3 USER STUDY 1: USABILITY AND EFFECTIVENESS OF VR-DOH

We present detailed subjective feedback from both experienced and novice participants below.

3.1 Semi-Structured Interview Results (Experts, P1-P6)

(1) Do you think the designs created using this tool align with your initial expectations?

P1 found the design mostly satisfactory, with minor areas for improvement. P2 stated that 80% of their expectations were fulfilled, with the pose being largely accurate, though fractures on the model surface hindered achieving a fully realized design. P3 expressed satisfaction with the details, particularly in the eyes of the SpongeBob model, and found the material texture consistent with the intended character image. P4 estimated that 70% of their expectations were met, as the realistic deformations matched their vision, but the finer details lacked completeness. Similarly, P5 found the results to align with their expectations despite minor fractures in the model. P6 noted that the outcome met basic expectations, though the initial design was not overly complex, and significant deformations led to fractures in the object.

(2) During your experience with the tool, what aspects were the most satisfying and the least satisfying? Additionally, what do you consider to be the greatest difficulty encountered while using the tool?

Most Satisfying: P1 highlighted the simplicity and enjoyment the tool brought to tasks, such as using a stick to create holes while designing strawberries, making the process feel immersive. The pinch gesture interaction using both hands was also found to be very practical. P2 appreciated the tool's ease of use without requiring extensive expertise, along with its high efficiency. The realistic deformation process, especially while editing the mermaid model, provided a visually engaging experience, akin to real swimming. Additionally, the ability to switch material parameters during editing was highly valued. P3 praised the intuitive interaction with 3D models, such as touching and squeezing, and also found the ability to adjust material parameters during editing particularly useful. P4 noted the tool's capability to provide real-time feedback on deformation with realistic rendering, which is often time-consuming in conventional modeling software. P5 found the tool effective for naturally and easily altering 3D model poses, with good continuity between joints, and appreciated the ease of adjusting movements and outfits to make designs more vivid. P6 valued the ability to merge objects seamlessly and highlighted the pinch gesture for shape editing without damaging surface details as especially useful.

Least Satisfying: P1 noted that the limited number of MPM simulation grids caused the texture of the strawberry object, which initially had a perforated texture, to become less apparent after merging. P2 expressed concern about potentially damaging the object too significantly during operations, which often led to surface fractures. P3 highlighted the absence of an undo function as a major limitation. P4 pointed out that the pinch gesture lacked proper visualization of the applied force, as well as recommended values for different materials and a clear indication of its maximum area of influence. P5 desired more detailed designs but found that insufficient particle counts made surfaces prone to fracturing. P6 also mentioned the lack of an undo function as a key drawback.

Greatest Difficulty: P1 found that the lack of tactile feedback made it challenging to adapt to deforming objects in a virtual reality environment, requiring some time to adapt to the new operational logic. P2 initially struggled with controlling the size of the selected area for the pinch gesture, leading to unsatisfactory results, but improved after multiple attempts. P3 identified difficulties in precisely adjusting the relative position of two merged objects using hands, as well as the issue of 3D Gaussian-based model surfaces easily fracturing. P4

noted that the pinch gesture lacked intuitive force control, making it hard to determine the appropriate force for different materials and avoid unexpected deformations. Additionally, 3D Gaussian-represented model surfaces were prone to breaking, with no automated surface repair function, and manual repairs proved difficult. P5 found it challenging to create symmetrical, streamlined shapes using hands. P6 highlighted the difficulty of precisely adjusting the relative position of two merged objects manually.

(3) What 3D modeling software do you use most frequently? How long have you been using it? Compared to that software, what do you think are the key differences between our tool and your preferred software? What are the respective advantages and disadvantages?

P1 highlighted the advantages of the tool, including its ability to make objects soft for modeling, allowing for more flexible and realistic deformations compared to setting control points manually in traditional software, although the manual method is more precise. Additionally, the system offers stronger realism, enabling users to see rendered changes during deformation and creating natural irregularities that better match real-world shapes. However, the flexibility comes at the cost of precision, and the system does not support splitting objects into two parts. P2 emphasized the tool's higher design efficiency compared to traditional modeling software, making it better suited for quickly expressing and brainstorming creative ideas. It also facilitates presentations and enhances communication with other designers. The ability to rotate perspectives and clearly view 3D models in a virtual reality environment is more intuitive than the traditional three-view method. P3 noted the stronger sense of immersion and the low learning curve, making it suitable for children. The real-time texture rendering during shape editing enhances the shape editing process. However, compared to traditional modeling software, the resulting objects are less detailed. P4 compared the tool to Blender, noting that the key advantage of the VR tool lies in its realism. However, Blender offers more diverse editing options, making it better suited for complex modeling needs. P5 discussed the fundamental difference in 3D modeling logic: traditional tools like 3DMax and ZBrush are mesh-based, requiring adjustments from points to lines to surfaces, while this system mirrors natural manipulation and plasticity, avoiding the need to learn internal operational logic. Advantages include intuitive and convenient operation, which better supports creative expression in 3D design, and realistic deformation without requiring rigging. Traditional tools struggle with deformation due to fixed meshes. However, this system is less capable of fine detailing compared to 3DMax, struggles with producing symmetrical, streamlined shapes, and assigns vertex colors directly, which negatively impacts rendering quality when modeling from scratch. P6 highlighted the low learning curve of the system, which allows users to achieve desired deformations quickly while benefiting from excellent real-time rendering. However, precise control is challenging, such as when adjusting the relative position of merged objects.

(4) What aspects do you find unsatisfactory, and do you have any suggestions for improvements? Are there any features you think should be added?

P1 suggested adding support for splitting objects into two parts and increasing the density of modeling objects to enhance surface detail during reconstruction. P2 recommended introducing a sculpting-style workspace with a fixed object position that only allows rotation along the y-axis, enabling the use of more precise tools, such as small chisels, for editing. They also suggested adding an undo function and providing the ability to repair 3D Gaussian-based model surfaces after fracturing. P3 proposed implementing a grid-based snapping feature when merging objects to counteract hand-tracking instability and ensure precise placement. They also suggested adding functionality to repair fractured 3D Gaussian-based model surfaces. P4 highlighted the need for more guidance on the appropriate force to apply to different materials and suggested adopting a pinch gesture mechanism similar to Blender's sculpting tools, where the applied force decreases as the area increases. They also emphasized the importance of enabling repairs for fractured 3D Gaussian-based model surfaces. P5 recommended adding an undo function, supporting the creation of symmetrical, streamlined shapes by smoothing nearby points, and introducing a feature to split objects into two parts. P6 proposed adding a grid-based snapping system for

precise positioning during object merging to mitigate the effects of hand-tracking instability. They also suggested reducing the likelihood of fractures in 3D Gaussian-based model surfaces.

3.2 Semi-Structured Interview Results (Novices, P7-P12)

(1) Do you think the designs created using this tool align with your initial expectations?

P7 observed minor discrepancies in physical properties but found the designs largely met expectations. P8 stated their projects generally met expectations. P9 found the outcomes satisfactory but saw room for improvement. P10 noted the results met expectations but merging objects was cumbersome. P11 expressed satisfaction with the watermelon model's results. P12 confirmed the designs met expectations.

(2) During your experience with the tool, what aspects were the most satisfying and the least satisfying? Additionally, what do you consider to be the greatest difficulty encountered while using the tool?

Most Satisfying: P7 found the intuitive operation, such as "modeling like clay," to be highly satisfactory due to its low learning curve. P8 appreciated the wide range of hands-on modeling options and material adjustments. P9 highlighted the tool's diverse and comprehensive features, including gravity-assisted functionality. P10 valued the high usability of the tool, noting its support for high frame rates and smooth real-time performance. P11 praised the freedom in detailed operations and the smooth functionality of basic features. P12 appreciated the realistic object rendering provided by the tool.

Least Satisfying: P7 noted performance issues such as insufficient particle numbers and surface material effects that need improvement. P8 highlighted the lack of split and undo functionalities. P9 pointed out imprecise hand tracking as a significant drawback. P10 mentioned that the object deformation behavior was overly sensitive, leading to accidental triggers. P11 expressed dissatisfaction with the limited primitive shape options. P12 observed that insufficient particle numbers caused positional errors after merging objects.

Greatest Difficulty: Hand-tracking issues were a recurring challenge, with imprecision, significant errors, and instability making position adjustments and operations difficult for users.

(3) From the perspective of usability (e.g., whether the tool is easy to learn and use), smoothness (e.g., whether operations are seamless and free from noticeable delays), realism (e.g., whether physical simulations of shape deformations meet your expectations), or any other aspects, please provide your feedback.

The tool was widely regarded as user-friendly, with low learning curves and easy-to-use interfaces across all participants (P7-P12). The system offered smooth and stable interactions with high frame rates, providing a seamless experience without noticeable lags or motion sickness (P7, P8, P10, P11, P12). In terms of realism, participants appreciated the adherence to physical rules and the overall accuracy in modeling (P8, P9, P10), though some noted areas for improvement, such as material diversity, detailed physical behaviors, and surface smoothing (P7, P8, P9, P11). Despite its strengths, hand-tracking performance was identified as a consistent issue, with imprecision and instability affecting precise operations and adjustments (P9, P12).

(4) What aspects do you find unsatisfactory, and do you have any suggestions for improvements? Are there any features you think should be added?

Suggestions for improvement included adding an undo function (P7, P9, P12), enhancing particle numbers for better surface reconstruction (P7, P12), and introducing more geometric presets like ellipsoids and rectangular prisms (P8, P12). Other proposals involved supporting single-dimensional shape adjustments (P9), optimizing hand-tracking, and improving collision box handling (P10). Participants also recommended adding object separation and text insertion (P8).

4 USER STUDY 2: COMPARISON WITH BLENDER

Below, we present detailed subjective feedback from our six participants.

4.1 Semi-Structured Interview Results

(1) What do you think are the key differences in operational experience between VR-Doh and Blender?

Participants highlighted several key differences between VR-Doh and Blender. P1 noted that VR-Doh’s 3D perspective makes macroscopic object shaping in a spatial environment more convenient, while Blender’s 2D perspective is better suited for detailed operations using a mouse. P2 emphasized that VR-Doh is easy to learn, with a simple operational logic that is highly accessible. Although its modeling logic may not be immediately clear, it becomes easy to understand after watching a tutorial, enabling one to know the next steps to take instinctively. However, the lack of tactile feedback makes fine control over objects more difficult. Blender, in contrast, has a higher learning curve but offers greater precision from a professional modeling perspective. P3 likened VR-Doh to the experience of working with real clay models, but noted its limitations in fine detail control, whereas Blender excels in precision. P4 observed that VR-Doh focuses on holistic, overall manipulation, while Blender is better for localized, detailed adjustments. Lastly, P5 pointed out that VR-Doh’s operations are more intuitive and easier to start, while Blender’s quantitative approach is more precise, reducing unintended errors. P6 noted VR-Doh does not require the abstraction of objects into vertices, edges, and surfaces for manipulation, whereas Blender necessitates the mental reconstruction of objects into vertices, edges, and surfaces in order to perform operations. Therefore, VR-Doh aligns more intuitively with the process of modeling objects

(2) What do you think are the key advantages and disadvantages of VR-Doh compared to Blender?

P1 highlighted that VR-Doh enables quick modeling using hands, efficiently realizing design concepts and avoiding the issue of “hands lagging behind the mind.” However, it has disadvantages in terms of precision during object shaping. P2 noted that while VR-Doh’s operations are more intuitive, its lack of precision makes it less suitable for professional users. Conversely, Blender offers higher precision but does not align well with habitual operations for modifying geometric objects. P3 emphasized VR-Doh’s intuitive usage but mentioned that it lacks fine operational control. Similarly, P4 observed that VR-Doh is more intuitive, with realistic physical deformation that corresponds to real-world experiences, but it struggles with fine object adjustments. Blender, in contrast, allows direct manipulation of the mesh for better geometric control, but it requires significant experience to use effectively, and its outputs may not align with physical realism. Lastly, P5 pointed out that VR-Doh facilitates quick comprehension of modeling tasks but is limited by its lack of precise control and the absence of an undo function. P6 found VR-Doh operates on a WYSIWYG (What You See Is What You Get) basis, eliminating the need for frequent switching between edit and render modes. However, the selected manipulation area in VR-Doh is relatively large, which limits the ability to precisely control what can or cannot be selected. Additionally, Blender offers a reversible modeling process through the use of Modifiers, enabling users to preview geometric changes without permanently altering the object.

REFERENCES

- Yiwen Chen, Zilong Chen, Chi Zhang, Feng Wang, Xiaofeng Yang, Yikai Wang, Zhongang Cai, Lei Yang, Huaping Liu, and Guosheng Lin. 2024. Gaussianeditor: Swift and controllable 3d editing with gaussian splatting. In *Proceedings of the IEEE/CVF Conference on Computer Vision and Pattern Recognition*. 21476–21485.
- Xinyu Gao, Ziyi Yang, Bingchen Gong, Xiaoguang Han, Sipeng Yang, and Xiaogang Jin. 2024. Towards Realistic Example-based Modeling via 3D Gaussian Stitching. *arXiv preprint arXiv:2408.15708* (2024).
- Yuanming Hu, Yu Fang, Ziheng Ge, Ziyin Qu, Yixin Zhu, Andre Pradhana, and Chenfanfu Jiang. 2018. A moving least squares material point method with displacement discontinuity and two-way rigid body coupling. *ACM Transactions on Graphics (TOG)* 37, 4 (2018), 1–14.
- Chenfanfu Jiang, Craig Schroeder, Joseph Teran, Alexey Stomakhin, and Andrew Selle. 2016. The material point method for simulating continuum materials. In *Acm siggraph 2016 courses*. 1–52.
- Bernhard Kerbl, Georgios Kopanas, Thomas Leimkühler, and George Drettakis. 2023. 3D Gaussian Splatting for Real-Time Radiance Field Rendering. *ACM Trans. Graph.* 42, 4 (2023), 139–1.
- Ben Mildenhall, Pratul P Srinivasan, Matthew Tancik, Jonathan T Barron, Ravi Ramamoorthi, and Ren Ng. 2021. Nerf: Representing scenes as neural radiance fields for view synthesis. *Commun. ACM* 65, 1 (2021), 99–106.

377 Deborah Sulsky, Shi-Jian Zhou, and Howard L Schreyer. 1995. Application of a particle-in-cell method to solid mechanics. *Computer physics*
378 *communications* 87, 1-2 (1995), 236–252.

379 Tianyi Xie, Zeshun Zong, Yuxing Qiu, Xuan Li, Yutao Feng, Yin Yang, and Chenfanfu Jiang. 2024. Physgaussian: Physics-integrated 3d
380 gaussians for generative dynamics. In *Proceedings of the IEEE/CVF Conference on Computer Vision and Pattern Recognition*. 4389–4398.

381

382

383

384

385

386

387

388

389

390

391

392

393

394

395

396

397

398

399

400

401

402

403

404

405

406

407

408

409

410

411

412

413

414

415

416

417

418

419

420

421

422

423